Scientific Journal of Impact Factor (SJIF): 5.71
e-ISSN (O): 2348-4470
p-ISSN (P): 2348-6406

International Journal of Advance Engineering and Research Development

International Conference on Momentous Role of Nanomaterials in Renewable Energy Devices

Volume 5, Special Issue 07, April-2018 (UGC Approved)

Enhanced Structural, surface morphological, optical and antibacterial activity of undoped and Ag doped $BiFeO_3$ nanopowders

A.T.Ravichandran[1], J.Srinivas[1,2*], A. Robert Xavier[3], R.Karthik[1],K.Dhanabalan[4],

[1]*PG & Research Department of Physics, National College (Autonomous), Tiruchirappalli, India.*
[2]*Department of Physics, Mount Zion College of Engineering and Technology, Pudukkottai, India.*
[3]*Department of Physics, Annai Veilankanni Arts and Science College, Thanjavur, India.*
[4]*PG & Research Department of Physics, J.J. College of Arts and Science College (Autonomous), Pudukkottai, India.*

Abstract - *$Bi_{(1-x)}Ag_{(x)}FeO_3$ where X=0.05, 0.10, and 0.15 at. % multiferroic were prepared by solution combustion method using urea as a fuel. The obtained product was calcined at the temperature of 550°C for 2 h in order to obtain pure phase. The XRD study reveals that the synthesized nanopowders exhibit rhombohedral structure and also confirm the decrease in the crystallite size as the dopant concentration increases. The FESEM micrograph shows that there are uniform grain size distributions without any agglomeration. The EDAX analysis shows the presence of Bi, Fe, O and Ag without any form of impurity peak. The PL shows high intense peak at 464 nm which is attributed for blue emission. The antibacterial activity of $BiFeO_3$: Ag nanopowders was found to be enhanced with increase in Ag doping level as it cause a reduction in the grain size.*

Keywords: *$BiFeO_3$, Ag, XRD, FESEM, HRTEM, PL*

I. INTRODUCTION

Multiferroic materials are those which exhibit both ferroelectric and magnetic ordering. These kinds of materials have potential applications for novel magneto electric devices and for exploring fundamental science in the coupling mechanism between electronic and magnetic order parameter [1-3] and between investigated intensively during the last decade. A wide variety of synthesis methods has been used in obtaining perovskite. The coupled magnetic and ferroelectric ordering have been proposed for various applications in solid oxide fuel cells, non –volatile magnetic memory devices, ultra sensitive magnetic read heads etc.[4-6]. Among all multiferroic materials studied so far $BiFeO_3$ which has simultaneously ferroelectricity, ferromagnetism and for ferroelasticity is the only known material exhibiting good ferromagnetism at room temperature [7]. It is one of the most discussed and controversial system of its high curie temperature of 1043 K and high Neel temperature of 647 K [8]. There are few obstacles in making good use of ceramics are (a) synthesis of pure material (b) getting highly remissive $BiFeO_3$ with low leakage current [9]. There are so many secondary phases like Bi_2O_3, $Bi_2Fe_4O_9$, Bi_25FeO_{39} are reported systematically.

There are different synthesis techniques have been reported such as solid state reaction [10-11], sol-gel method [12-13] microwave hydrothermal [14-15] chemical precipitation [16] sonochemical [17] solution combustion [18] and so on. Each method has their own advantages and limitations and the main purpose behind each synthesis is to obtain the highest purity with simple recipe with low possible temperature [19]. Of all the various techniques combustion is found to be versatile, simple and rapid process which allows effective synthesis of a verity of materials [20]. This is based on the mixing of reactants which can be oxidised easily such as fuels trigger a self sustained exothermic redox reaction. Hence in this paper we described in detail urea assisted combustion techniques at a relatively normal temperature. Characteristics, morphology, reaction mechanism of $BiFeO_3$ discussed.

II. EXPERIMENTAL PROCEDURE

A. Preparation of undoped and Ag doped $BiFeO_3$

$BiFeO_3$ and Ag doped $BiFeO_3$ was synthesized via solution combustion technique, using $Bi(NO_3)_3.5H_2O$, $Fe(NO_3)_3.9H_2O$ and Urea. $Ag(NO_3)$ was added by $Bi_{(1-x)}Ag_{(x)}FeO_3$ with different values of 'x' ranging as x=0, 0.05, 0.1, 0.15 composition along with the pure $BiFeO_3$. Stoichiometry ratios of all were mixed and kept in the preheated muffle furnace of 500˚C. The solution gets heated and boiled with the evaluation of large amount of gases. At certain point all water gets evaporated and at final stage its gets ignited with lot of heat and results into a burning solid. Additionally, the sample was calcined at 550˚C for 2 h.

B. Characterization techniques

The crystalline structure of the calcined powders was examined by an X-ray diffractometer (PANalytical-PW 340/60 X' pert PRO) using Cu-Kα radiation (λ=1.5406 Å). The nanostructure of the powders was investigated by a transmission electron microscope (TEM, Hitachi H-7100). The morphology was done with FESEM (Hitachi SU8000) coupled with EDAX (JEOL-JSM 6390 with attachment INCA-Penta FETX3 OXFORD). The photoluminescence property is also determined (JobinYvon_FLUROLOG-FL3-11).

C. Evaluation of antibacterial performance

The antibacterial property of Ag+ $BiFeO_3$ nanopowders were analyzed by their zone of inhibitions for two gram negative (Escherichia coli, Klebsiellapneumoniae) and two gram positive (Staphylococcus aureus, Bacillus subtilis). An overnight culture of each microorganism was adjusted to an OD of 0.1 and swabbed onto Mueller Hilton agar plates. Using a cork borer, holes were punched on the agar, followed by addition of the stock solutions containing synthesized nanopowders (10µg/mL). These plates were incubated at 37˚C for 24 h and the zone of inhibitions was measured in diameter.

III. RESULTS AND DISCUSSION

A. Structural studies

The XRD pattern of the undoped and Ag doped $BiFeO_3$ is shown in the Fig.1. All the peaks can be well indexed (JCPDS card no.86-1518) on the basis of $R3_C$ structure [21-22]. The average crystallite sizes (D) of the powder were calculated from the full width at half maximum of the characteristic diffraction peaks from the major reflection using Debye-Scherrer formula.

$$D=0.9\lambda/\beta \cos \theta\text{----------}(1)$$

Where λ is the wavelength of the X-ray used,β is the broadening of the diffraction peak at half of its maximum intensity (i.e,Full width half maximum-FWHM) θ is the Bragg's angle. It is found that from the formula the crystallite size varies from 56 nm to 46 nm.

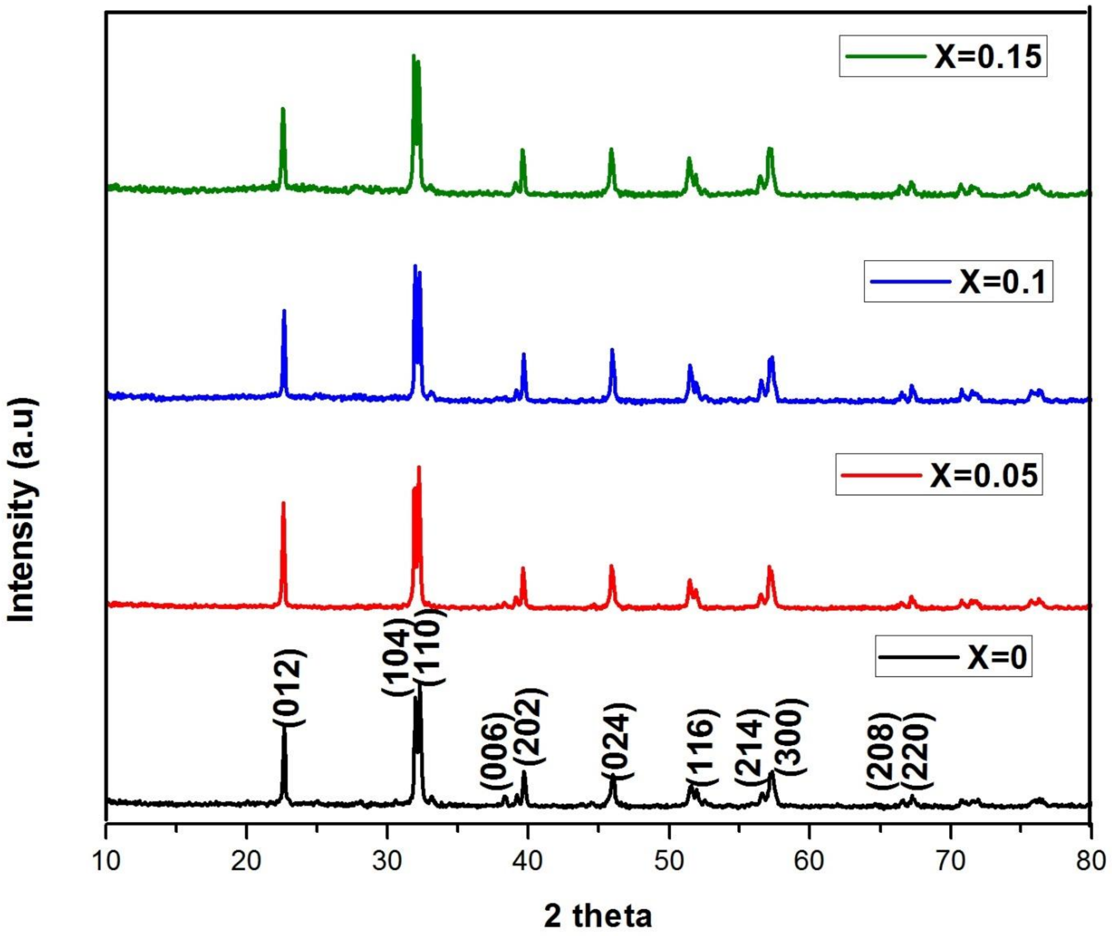

Figure 1.The XRD pattern of the undoped and Ag doped $BiFeO_3$ ($Bi_{(1-x)}Ag_{(x)}FeO_3$ where X=0.05, 0.10, and 0.15 at. %)

B. Morphology

Fig 2(a-d) shows the FESEM of $BiFeO_3$ and Ag doped BiFeO3 shows that there are uniform grain size distribution. Some particles adhere to large ones indicating the growth of the $BiFeO_3$ and that can be due to Ostwald ripening mechanism [23]. Besides the Fig. there are formations of nano wires which may be due to the catalysed reaction process involved very high local temperature. More over the obtained powders are pure rhombohedral $BiFeO_3$ phase without orthorhombic phase. Fig.3 shows the EDAX analysis and it has the presence of Bi, Fe, O and Ag respectively.

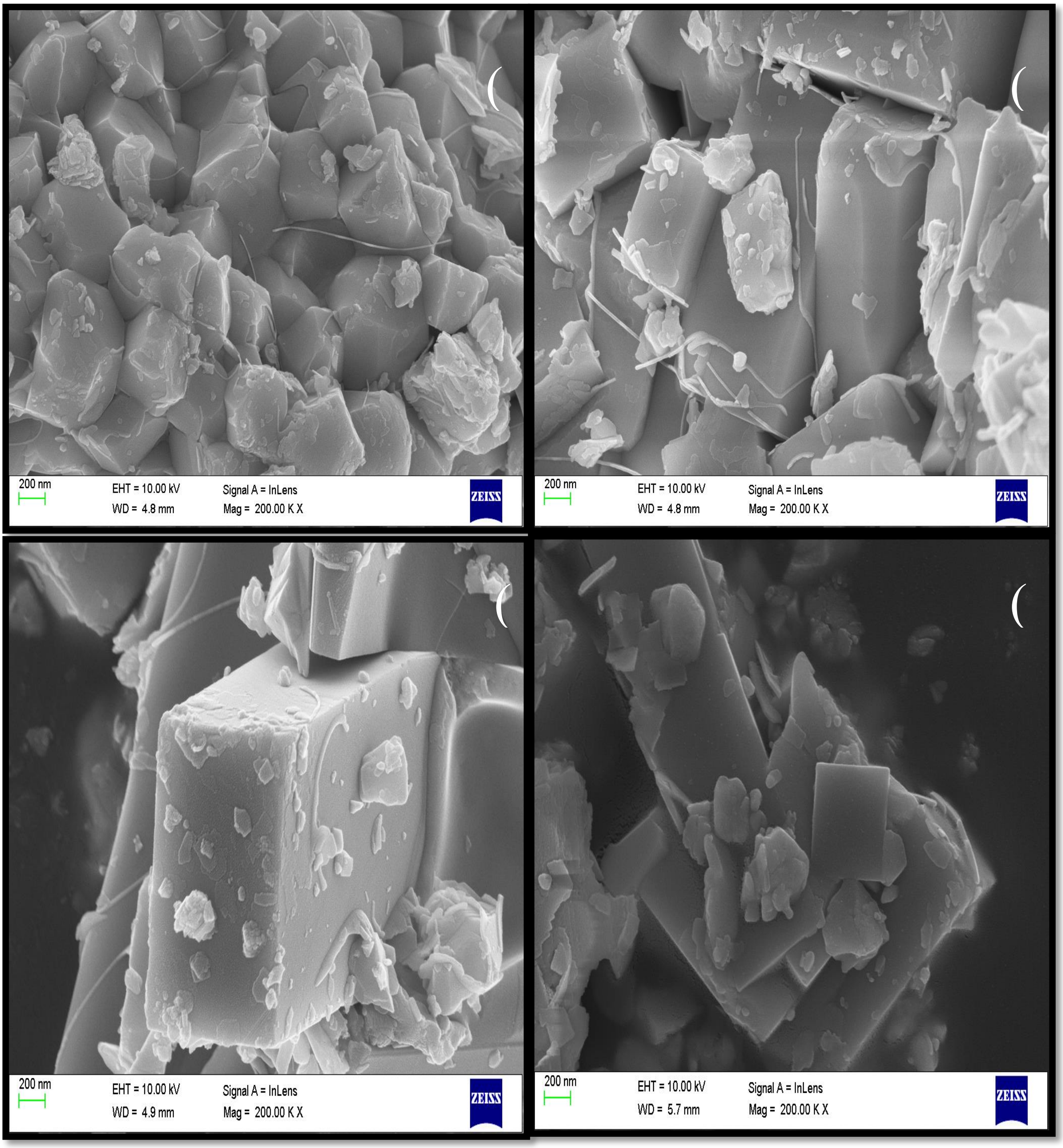

Figure 2(a-d). FESEM images of $BiFeO_3$ and Ag doped $BiFeO_3$ ($Bi_{(1-x)}Ag_{(x)}FeO_3$ where X=0.05, 0.10, and 0.15 at. %)

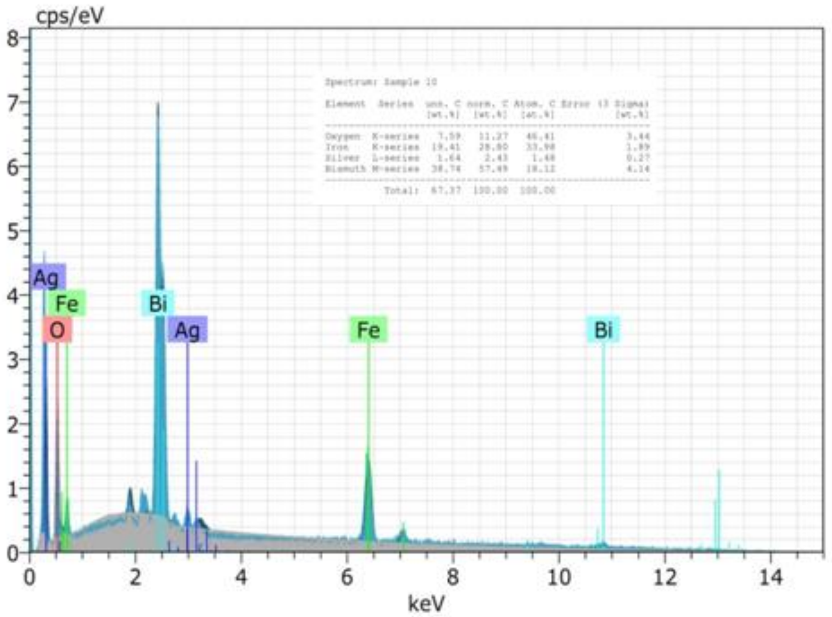

```
Spectrum: Sample 10

Element  Series   unn. C norm. C Atom. C Error (3 Sigma)
                  [wt.%]  [wt.%]  [at.%]          [wt.%]
---------------------------------------------------------
Oxygen  K-series   7.59   11.27   46.41            3.44
Iron    K-series  19.41   28.80   33.98            1.89
Silver  L-series   1.64    2.43    1.48            0.27
Bismuth M-series  38.74   57.49   18.12            4.14
---------------------------------------------------------
           Total: 67.37  100.00  100.00
```

Figure 3. Shows the EDAX analysis ($Bi_{(1-x)}Ag_{(x)}FeO_3$ where X=0.05, 0.10, and 0.15 at. %)

C. Optical studies

The nature of the transmittance and the band gap of the nano powders are estimated from Tauc's relation connecting the absorption co-efficient (α) and the photon energy (hν). The direct band gap for various concentrations is determined by extrapolating the straight line portions to the energy axis are shown in Fig.4. The band gap values for undoped and Ag doped $BiFeO_3$ for various doping concentration x=0, x=0.05, x=0.10 and x=0.15 are estimated to 1.44, 1.51, 1.55 & 1.58 respectively. It's obvious from the result the optical band gap increases with increases of doping concentration which may be due to the quantum size effect.

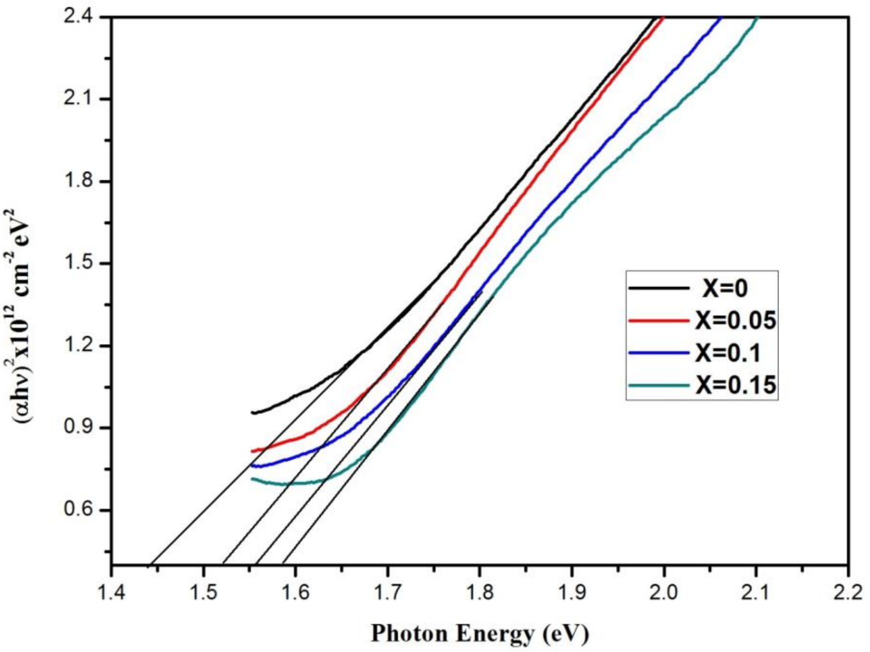

Figure 4. The direct band gap for various concentrations the undoped and Ag doped $BiFeO_3$ ($Bi_{(1-x)}Ag_{(x)}FeO_3$ where X=0.05, 0.10, and 0.15 at. %)

D. Photoluminescence (PL) spectra

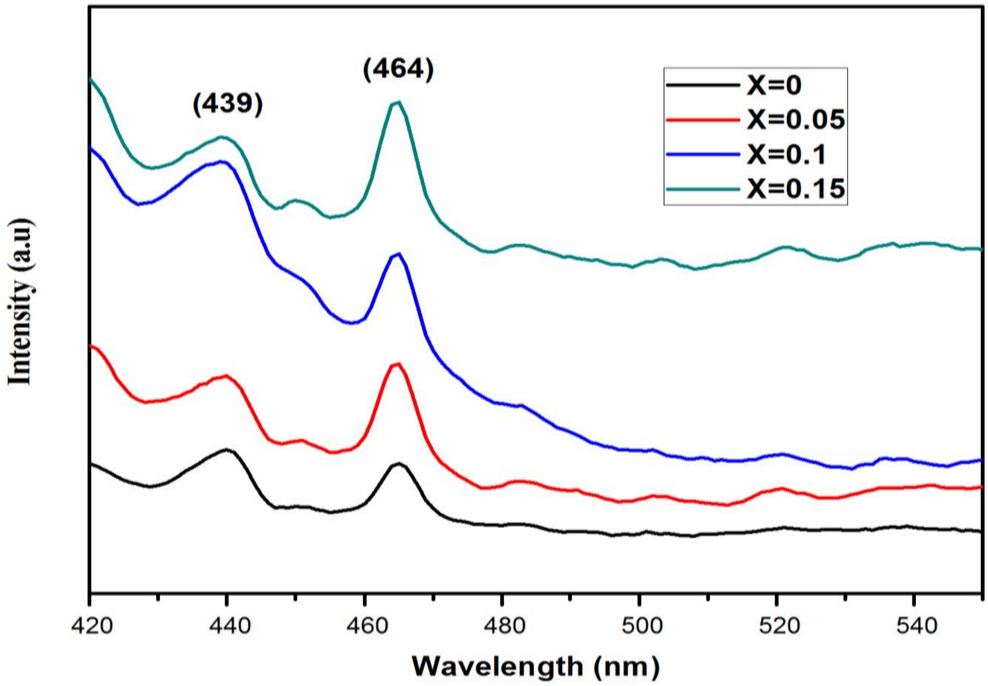

Figure 5. photoluminescence spectra of undoped and Ag doped $BiFeO_3$ ($Bi_{(1-x)}Ag_{(x)}FeO_3$ where X=0.05, 0.10, and 0.15 at. %)

Fig.5 shows the photoluminescence spectra of undoped $BiFeO_3$ and Ag doped $BiFeO_3$ nanopowders. The presence of small peak at 439 nm confirms the emission of violet emission. The sharp peak at 464 nm is attributed to the blue emission. The asymmetric property occurs probably due to surface oxygen vacancies that consequently results in several functions below the conduction band. As per the earlier reference on $BiFeO_3$ the luminescence around λ=451 nm to λ=464 nm corresponds to the characteristics bond edge emission wherever peak at 464 n is attributed to the NBE due to various defect trap within the band gap.

E. Antibacterial activity

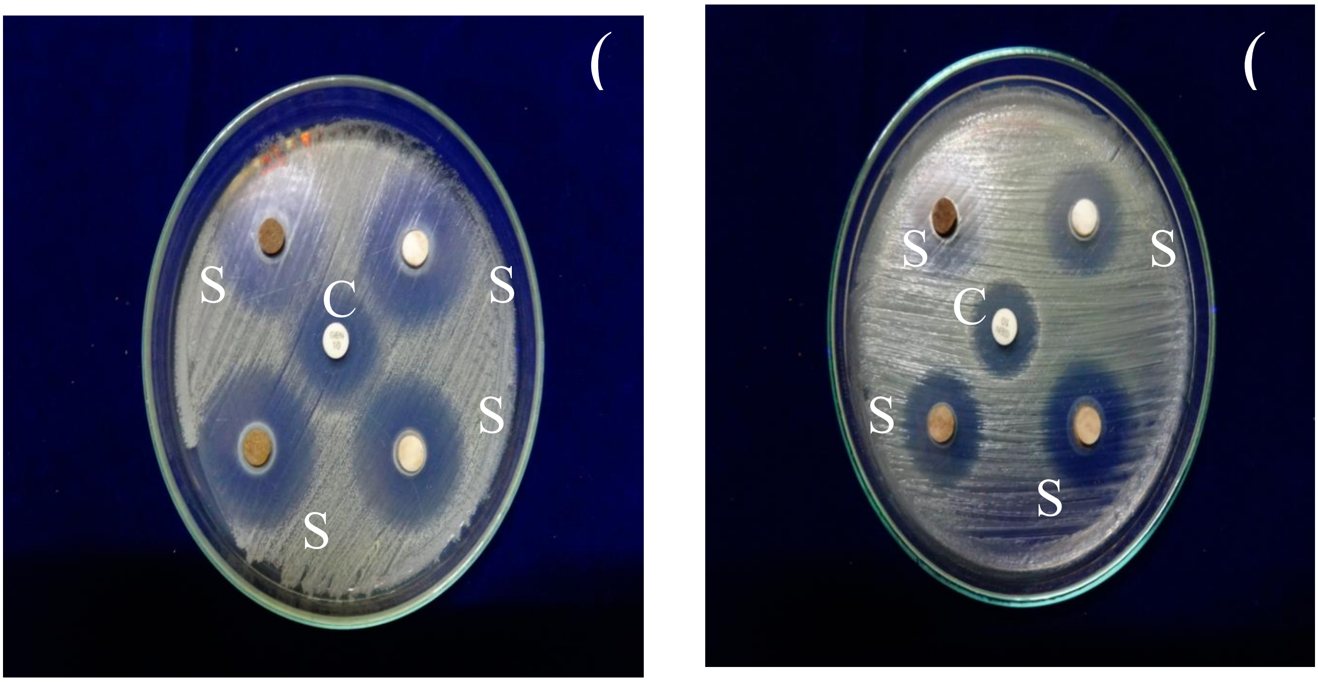

Figure 6. The antibacterial activity of undoped and Ag doped $BiFeO_3$ against a) Klebsiellapneumoniae and b) Staphylococcus aureus. ($Bi_{(1-x)}Ag_{(x)}FeO_3$ where X=0.05, 0.10, and 0.15 at. %)

Fig.6(a-b) shows the antibacterial activity of undoped and Ag doped $BiFeO_3$ nanopowders were investigated against gram negative (Klebsiellapneumoniae) and gram positive (Staphylococcus aureus) bacterial strains respectively. It is been noted that there is no zone of inhibition over the control. The variation in the diameter of the zone of inhibition is platted in the bar diagram (Fig.7). Ag doped $BiFeO_3$ influences higher antibacterial activity than that of undoped nanopowders. The particle size of the samples play crucial role in the antibacterial activity of synthesized nanopowder. As can be seen the zone of inhibition increases with increase in the dopant ratio.

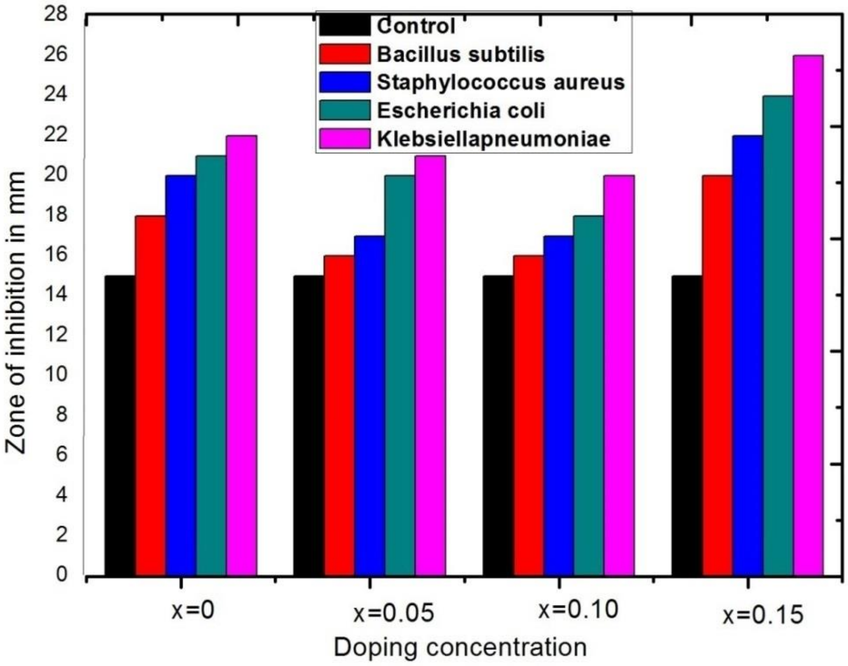

Figure 7. The antibacterial activity of undoped and Ag doped $BiFeO_3$ ($Bi_{(1-x)}Ag_{(x)}FeO_3$ where X=0.05, 0.10, and 0.15 at. %)

When Ag is doped with $BiFeO_3$, the substitution of Ag^+ ions into Bi^{3+} sites make more numbers of Bi ions to occupy the interstitial position as the ionic radii of Ag^+(0.126nm) is higher than that of Bi^{3+}(0.096). The presence of these Bi^{3+} ions is confirmed through PL studies.

IV CONCLUSION

Undoped and Ag doped $BiFeO_3$ nanopowders prepared using solution combustion method. It has been found that the average size of the grains decrease with the increase in the doping level. The blue emission peak of the PL spectra conform the proper substitution of Ag ions in to Bi and Fe sites in $BiFeO_3$ lattice. It has been found that the $BiFeO_3$ nanopowders doped with 0.15 at % of Ag exhibit higher antibacterial efficiency against Klebsiellapneumoniae compares with other samples.

REFERENCE

[1]. N. Hur, S. Park, P.A. Sharma, J.S. Ahn, S. Guha, S.W. Cheong, “Electric polarization reversal and memory in a multiferroic material induced by magnetic fields” *Nature*, 429, 392–395, 2004.
[2]. N.A. Spaldin, M. Fiebig, “The Renaissance of Magnetoelectric Multiferroics”, *Science*, 309, 391–392, 2005.
[3]. G.A. Smolenskii, I. Chupis, Sov. “Ferroelectromagnets” Phys. Usp. 25, 475–493, 1982.
[4]. T. Hibino, S. Wang, S. Kakimoto, M. Sano, “One-chamber solid oxide fuel cell constructed from a YSZ electrolyte with a Ni anode and LSM cathode” *Solid State Ionics*, 127 , 89–98, 2000.
[5]. A. Moser, C.T. Rettner, M.E. Best, E.E. Fullerton, D. Weller, M. Parker, M.F. Doerner, “Writing and detecting bits at 100 Gbit/in/sup 2/ in longitudinal magnetic recording media” *IEEE Transactions on Magnetics*, 36 , 2137–2139, 2000.
[6]. S.S.P. Parkin, K.P. Roche, M.G. Samant, P.M. Rice, R.B. Beyers, R.E. Scheuerlein,E.J. O’Sullivan, S.L. Brown, J. Bucchigano, D.W. Abraham, Yu Lu, M. Rooks,P.L. Trouilloud, R.A. Wanner, W.J. Gallagher, “Exchange-biased magnetic tunnel junctions and application to nonvolatile magnetic random access memory (invited)” *Journal of Applied Physics*, 85, 5828–5833,1999.

[7]. Tie Li, Jianfeng Shen,,Na Li, Mingxin Ye, "One-pot self-catalyzed synthesis and properties of multiferroic $BiFeO_3$ single-phase crystallites by sucrose-assisted combustion", *Journal of Alloys and Compounds*, 548, 89-95, 2013.

[8]. P. Fischer, M. Polomska, I. Sosnowska, M. Szymariski, "Temperature dependence of the crystal and magnetic structures of $BiFeO_3$", *J. Phys. Chem. C*, 13, 1931–1940, 1980.

[9]. R. Mazumdera, A. Senb," Effect of Pb-doping on dielectric properties of $BiFeO_3$ ceramics" J. Alloys Comp. 475, 577–580, 2009.

[10]. H. Ke, W. Wang, Y.B. Wang, H.J. Zhang, D.C. Jia, Y. Zhou, "Dependence of dielectric behavior in $BiFeO_3$ ceramics on intrinsic defects" *J. Alloys Comp.* 541, 94–98, 2012.

[11]. M.S. Bernardo, T. Jardiel, M. Peiteado, A.C. Caballero, M. Villegas, "Reaction pathways in the solid state synthesis of multiferroic BiFeO3" *J. Euro, Ceram. Soc.* 31, 3047–3053, 2011.

[12]. J. Zhang, M.A. Gondal, W. Wei, T.N. Zhang, Q.Y. Xu, K. Shen, "Preparation of room temperature ferromagnetic $BiFeO_3$ and its application as an highly efficient magnetic separable adsorbent for removal of Rhodamine B from aqueous solution", *J. Alloys Comp*. 530, 107–110, 2012.

[13]. L.R. Luo, W. Wei, X.Y. Yuan, K. Shen, M.X. Xu, Q.Y. Xu, "Multiferroic properties of Y-doped $BiFeO_3$", *J. Alloys Comp.* 540, 36–38, 2012.

[14]. Z. Wang, J.Y. Zhu, W.F. Xu, J. Sui, H. Peng, X.D. Tang, "Microwave hydrothermal synthesis of perovskite $BiFeO_3$ nanoparticles: An insight into the phase purity during the microwave heating process", *Mater. Chem. Phys.* 135, 330–333, 2012.

[15]. A.Y. Kim, S.H. Han, H.W. Kang, H.G. Lee, J.S. Kim, C.I. Cheon, "Dielectric and magnetic properties of $BiFeO_3$ ceramics prepared by hydrothermal synthesis".Ceram. Int. 38, 397–401, 2012.

[16]. S. Farhadi, N. Rashidi, "Microwave-induced solid-state decomposition of the Bi[Fe(CN)6]·5H2O precursor: A novel route for the rapid and facile synthesis of pure and single-phase BiFeO3 nanopowder", *J. Alloys Comp.* 503, 439–444, 2010.

[17]. N. Das, R. Majumdar, A. Sen, H.S. Maiti, "Nanosized bismuth ferrite powder prepared through sonochemical and microemulsion techniques". *Mater. Lett.* 61, 2100–2104, 2007.

[18]. X.B. He, L. Gao, "Synthesis of pure phase BiFeO3 powders in molten alkali metal nitrates", *Ceram. Int.* 35, 975–978, 2009.

[19]. A. Jawad, A.S. Ahmed, S.S.Z. Ashraf, M. Chaman, A. Azam, J. Exploring the dielectric behaviour of nano-structured Al3+ doped BiFeO3 ceramics synthesized by auto ignition processAlloys Comp. 530, 63–70, 2012.

[20]. Y.G. Jun, X.C. Li, J.Y. Zhou, Y. Tang, Y.M. Zhang, Y.W. Li, "Factors controlling pure-phase magnetic $BiFeO_3$ powders synthesized by solution combustion synthesis", *J. Alloys Comp.* 509, 9271–9277, 2011.

[21]. P. Fischer, M. Polomskya, I. Sosnowska, M. Szymanksi, "Temperature dependence of the crystal and magnetic structures of BiFeO3", *J. Phys. C*, 13, 1931-1980.

[22]. J.D. Bucci, B.K. Robertson, W.J. James, "The precision determination of the lattice parameters and the coefficients of thermal expansion of $BiFeO_3$",*J. Appl. Crystallogr.* 5, 187, 1972.

[23]. S. Ghosh, S. Dasgupta, A. Sen, H.S. Maiti, "Low-Temperature Synthesis of Nanosized Bismuth Ferrite by Soft Chemical Route", *J. Am. Ceram. Soc*. 88 , 1349– 1352, 2005.